JOURNAL OF CATALYSIS **160,** 65–75 (1996)
ARTICLE NO. 0124

A Surface Science Investigation of Methanol Synthesis over a Zn-Deposited Polycrystalline Cu Surface

J. Nakamura,* I. Nakamura,* T. Uchijima,* Y. Kanai,† T. Watanabe,† M. Saito,‡ and T. Fujitani‡

*Institute of Materials Science, University of Tsukuba, †Research Institute of Innovative Technology for Earth, and ‡National Institute for Resources and Environment, Tsukuba, Ibaraki 305, Japan

Received March 17, 1995; revised October 23, 1995; accepted January 23, 1996

The hydrogenation of CO_2 over a Zn-deposited polycrystalline Cu surface was performed at 523 K and 18 atm using a high-pressure reactor combined with an XPS–AES apparatus. It was clearly shown that ZnO_x species formed on the Cu surface during the reaction directly promoted the methanol formation activity, indicating the creation of active sites except for Cu^0. At optimum Zn coverage ($\Theta_{Zn} = 0.17$) the Zn-deposited Cu surface was sixfold more active than the Zn-free Cu surface for methanol formation. The turnover frequencies (TOF) increased with Zn coverage below $\Theta_{Zn} = 0.17$ and decreased above $\Theta_{Zn} = 0.17$. The TOF and the activation energy for methanol formation over the Zn-deposited Cu were in fairly good agreement with those for the Cu/ZnO powder catalysts. Thus, the Zn-deposited Cu surface can be regarded as a model of Cu/ZnO catalysts. The postreaction surface analysis by XPS, after evacuation of the reaction mixture at 523 K, showed the formation of ZnO_x species with a Zn/O ratio of about unity at any Zn coverage. Formate species was observed on the postreaction Cu surface in the presence of the ZnO_x species. The amount of the formate species increased with Θ_{Zn} below $\Theta_{Zn} = 0.2$ and then slightly decreased at $\Theta_{Zn} > 0.2$.

I. INTRODUCTION

Methanol synthesis over Cu/ZnO-based catalysts by the hydrogenation of $CO/CO_2/H_2$ has been the subject of much controversy in spite of the huge amount of research performed for some decades. Much has been reported on the active species of Cu, the role of ZnO, the kinetics, and the mechanism (1–3). Several surface science studies using single crystals of Cu or ZnO with respect to the methanol synthesis have also carried out for modeling Cu catalysts at relatively high pressures.

Regarding the active sites, evidence that Cu^{n+} is the pivotal catalytic species for methanol formation has been presented using surface analysis techniques. Szanyi and Goodman (4) have reported that the methanol synthesis activity of an oxidized Cu(100) surface was higher than that of an oxygen-free Cu(100) by a factor of two and concluded that the very low activity of clean Cu(100) was attributed to a low concentration of ionic copper. Sheffer and King (5) have shown that the activity for methanol synthesis from CO over unsupported copper catalysts increases with the concentration of Cu^+ sites stabilized by alkali compounds. On the other hand, some researchers have reported that metallic Cu is the active species for the methanol synthesis (6–9). Chorkendorff and co-workers (9) have shown that metallic Cu is the active catalyst in the methanol synthesis from CO_2 and H_2 over Cu(100). It has also been reported that the reactivity of Cu particles deposited on the ZnO single-crystal surfaces has been found to be different depending on the surface planes such as (0001), $(000\bar{1})$, and $(10\bar{1}0)$ (10, 11).

The synergy effect of ZnO and Cu on the catalytic activity has been reported by several researchers (12–14), although some researchers deny the synergy effect by showing the linear relationship between the copper metal surface area and the methanol synthesis activity (8). Burch and co-workers (12, 13) have admitted the synergy between Cu and ZnO for the methanol synthesis by confirming the promotion of the catalytic activity upon mixing Cu/SiO_2 with ZnO/SiO_2. They have further proposed a model for the role of ZnO: ZnO acts as a reservoir for spillover hydrogen and reverse spillover accelerates the methanol synthesis reaction on Cu. On the other hand, we (15–17) have recently reported that the support effect including the role of ZnO can be well explained by the creation of active sites, Cu^+ species, stabilized by the metal oxide. That is, the mountain-shaped correlation curve between the specific activity of methanol formation and the oxygen coverage on Cu for the postreaction Cu surface was obtained for Cu-based catalysts containing various metal oxides (15). This suggests that Cu^+ and Cu^0 species are both essential for the methanol formation. Further, migration of ZnO_x from ZnO particles onto the Cu surface has been observed upon reduction of Cu/ZnO (16) and $Cu/SiO_2 + ZnO/SiO_2$ mixtures (17); thus, it was concluded that Cu^+ is stabilized by the ZnO_x species that migrated from the ZnO particles onto the Cu surface, leading to formation of a Cu^+-O-Zn active site.

Here, we report the results of the surface science investigation of methanol synthesis by hydrogenation of CO_2

0021-9517/96 $18.00

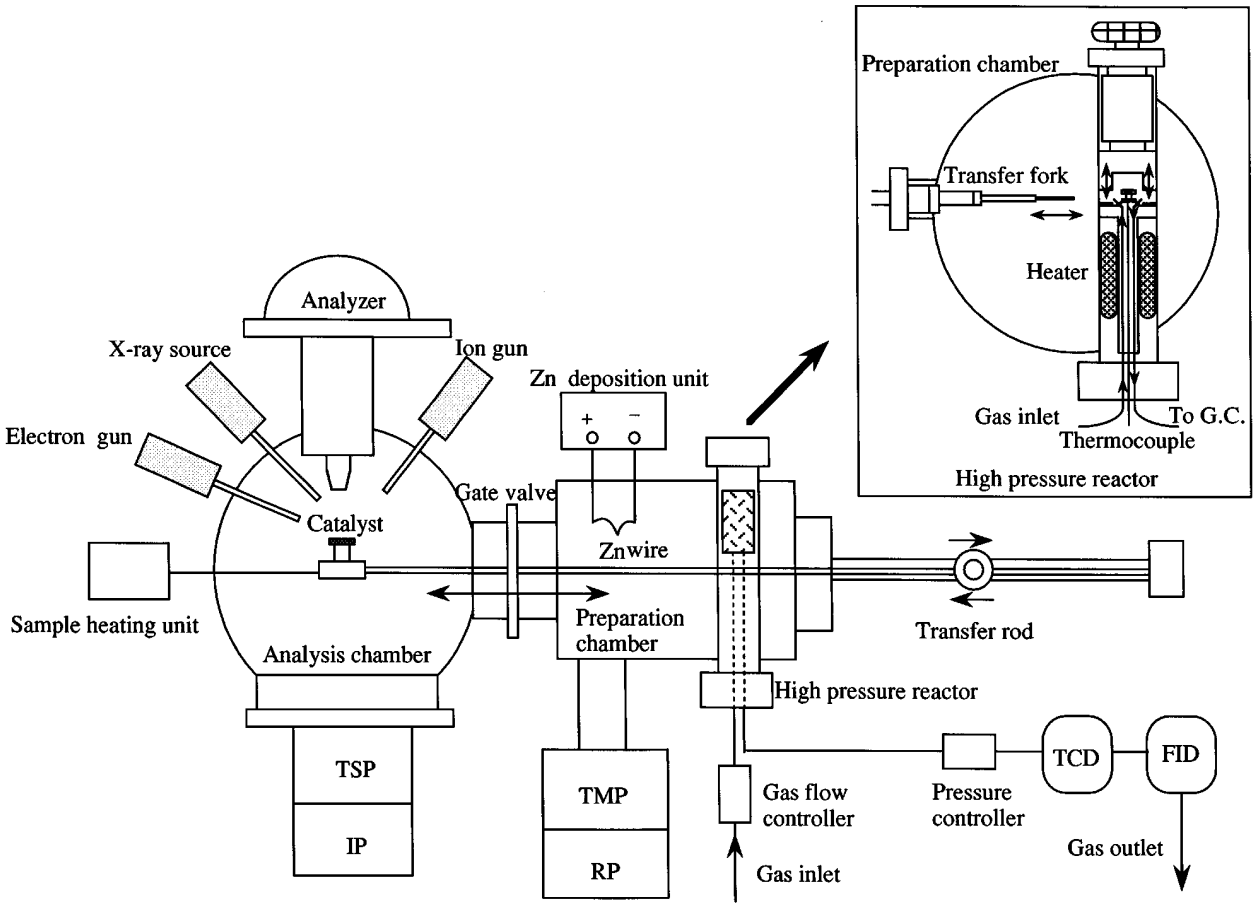

FIG. 1. Schematic diagram of the UHV apparatus.

over a Zn-deposited Cu polycrystalline surface to prove the proposed ZnO_x-promotional model based on our previous results.

II. EXPERIMENTAL

The experiments were carried out in a UHV apparatus (VG-ESCALAB-220i) as depicted in Fig. 1, where a UHV chamber for surface analysis was combined with a high-pressure flow reactor for catalytic reactions. The UHV chamber was equipped with a hemispherical energy analyzer for X-ray photoelectron spectroscopy (XPS) and Auger electron spectroscopy (AES), an ion gun for Ar^+ sputtering, and a sample heating unit. The chamber was pumped with an ion pump and a titanium sublimation pump, and the base pressure was less than 2×10^{-10} Torr. High-pressure reactions (18 atm) were run in the flow reactor ($\sim$4.5 cm^3) at a total flow rate of 5.56 cc/min ($H_2/CO_2 = 3$, 100 cc/min at 1 atm), and the reactants and products were analyzed by on-line gas chromatographs with a thermal conductivity detector (TCD) and a flame ionization detector (FID). A silica capillary column (Shimadzu CBP20, 25 m, 0.25 $\mu\phi$) and Porapak Q column (3 m) were used for the separation of CH_3OH/CH_4 and CO_2/CO, respectively. The reactor was pressurized by a pressure-control valve connected to the reactor downstream. The pressure at the inlet of the reactor was measured with a high pressure gage. The pressure in the gas line between the pressure-control valve and the gas chromatographs was 1 atm. The gas line between the reactor and the gas chromatograph was heated at 383 K using a tape heater to eliminate the condensation of methanol on the wall of the stainless steel tubes. The reactor consisted of a cylinder with a window through which a sample holder could be transferred between the reactor and a preparation chamber and was enclosed by a partition to fix the sample holder and a valve moving downward through the cylinder the seal the window using a cup-shaped component. The cylinder went through the preparation chamber (base pressure, $\sim 10^{-7}$ Torr), in which a heater and chromel–alumel thermocouple for controlling the sample temperature were attached to the rear side of the sample holder. The heater located below the sample holder allowed the sample to be heated up to 700 K while reactant gases were passed through the reactor. A Eu-

rotherm temperature controller used in this study was calibrated in advance by measuring the exact sample temperature, where the sample was directly connected to a thermocouple. As an example, the sample temperature was 523 K when the temperature of the bottom of the sample holder was 543 K. The sample holder was allowed to be transferred between the reactor, the preparation chamber, and the analysis UHV chamber using a transfer rod and manipulator called a transfer fork. The UHV analysis chamber and the preparation chamber were partitioned by a gate valve.

The Cu polycrystal (99.9999%) was a square foil (10 mm × 10 mm × 1 mm), polished with diamond paste to a mirror finish, and mounted on the sample holder mechanically using small Ni foils (3 mm × 5 mm) spot-welded on the sample holder. During the course of this investigation, the sample was repolished several times, and the results of the kinetic measurements were reproduced after repolishing. The front sample surface was routinely Ar^+-sputter cleaned at 300 and 723 K and subsequently followed by annealing at 723 K for ~10 min. No catalytic activity for methanol formation was observed without the sample cleaning procedure. After cleaning the sample, the activity for methanol formation correlated well and reproducibly with the Zn coverage. Based on these data, it was concluded that the methanol formation reaction occurred almost entirely on the front surface, and the back surface was passivated by segregated impurities. As the reactants, 99.999% pure CO_2 and H_2 were used without further purification.

The sample was cleaned and characterized by XPS or AES in the UHV chamber and then translated to the preparation chamber, where zinc was vapor-deposited on the front surface of the sample by resistively heating a Zn wire (0.27 mm diameter, 99.99%) located ~2 cm away from the sample. The Zn-deposited Cu sample was characterized by XPS or AES to estimate the coverage of Zn. The sample was then transferred to the evacuated reactor, which was then closed and pressurized with CO_2 and H_2. After heating the sample near the reaction temperature, the reactant was introduced to the reactor, and then the reaction temperature was adjusted. The reaction was traced using the gas chromatographs for at least 60 min. After the reaction, the applied heat was turned off, and the reactant mixture was then evacuated, while the sample temperature was still maintained at the reaction temperature without heating. The sample was then analyzed by XPS for postreaction surface analysis.

XPS spectra were measured with Mg $K\alpha$ radiation at a pass energy of 50 eV. The full-width at half maximum (FWHM) at the pass energy was 2.1 eV for a Cu 2p peak for the polycrystalline Cu sample. The spectra were referenced to the Fermi level, which gives Cu $2p_{3/2}$ and Ag $3d_{5/2}$ peaks at 932.4 and 367.9 eV binding energy (BE) for metallic Cu and Ag samples, respectively. The AES and XPS spectra were collected by detection normal to the surface. The coverage $\Theta = 1$ was defined as the number of Cu surface atoms (1.7×10^{15} atoms/cm^2), which was assumed to be similar to that for Cu(111), 1.77×10^{15} atoms/cm^2. The oxygen coverage on the Cu surface was estimated to be $\Theta_O = 0.5$ for the oxidized Cu surface by O_2 at 600 K and 5×10^{-5} Torr for 40 s, giving a O(KVV)/Cu(LVV) peak-to-peak AES ratio of 0.13, which is in good agreement with the literature data (18). The Zn coverage was then estimated from the integrated O 1s : Zn $2p_{3/2}$ XPS intensity ratio using the sensitivity factors of 0.63 for O1s and 5.3 for Zn $2p_{3/2}$.

The stainless steel walls of the reactor were found to be active for methanol formation, methanation reaction, and the reverse water–gas shift reaction in the blank test. Also, significant carbon deposits were seen near the sample holder. Thus, the wall inside the reactor was coated with Au (1 μm)/Cr (2 μm), which lessened the catalytic activities as well as carbon deposition significantly. The catalytic activity of the reactor for methanol formation was further retarded by heating the reactor wall at ~500 K. Normally, the amounts of methanol and CO catalyzed by the wall material are less than 10 and 20 of those formed on the Cu sample, respectively. The amount of methane formed by the hydrogenation of CO was of the same order as that of methanol, which was independent of the coverage of Zn on the Cu surface. In each kinetic measurement for the methanol synthesis, the blank tests, i.e., reaction without the Cu sample, were carried out to eliminate contribution of the catalytic activity of the material except for the Cu sample.

The activity of the Zn-deposited Cu surface was evaluated in terms of turnover frequency (TOF) defined as the number of product molecules formed on a Cu atom per sec (molecules/site s). The yield of methanol was first calculated by the equation

$$\text{Yield} = X_{CH_3OH}/(X_{CO} + X_{CO_2} + X_{CH_4} + X_{CH_3OH}),$$

where X was the concentration of products and reactant containing carbon. The TOF was then calculated from the yield using

$$\begin{aligned}\text{TOF} = {} & \text{Yield} \times 0.42\ (\text{cc/s, for } CO_2) \times 6.02 \times 10^{23} \\ & (\text{molecules /mol})/[24400\ (\text{cc/mol, for 1 atm, 298K}) \\ & \times 1.7 \times 10^{15}\ (\text{sites/cm}^2)],\end{aligned}$$

where the ideal gas law was used assuming very low conversion.

In comparison, kinetic measurements of CO_2 hydrogenation over powder Cu/ZnO (50/50, by weight), Cu/SiO_2(30/70), and Cu/Ga_2O_3(50/50) catalysts and the measurements of oxygen coverage on the surface of the Cu particles were also carried out under the same pressure condition (18 atm) as the reaction over the ZnO_x/polycrystalline Cu, which were the same experiments as reported previously except

for the pressure condition (50 atm) (15, 16). The experimental apparatus used in this study and the procedures have been described elsewhere (15). Briefly, a flow reactor for high-pressure reactions (up to ~80 atm) was connected to the instruments of the reactive frontal chromatography (RFC) for measuring the oxygen coverage on the Cu surface. After the hydrogenation of CO_2 at 18 atm, which was the same pressure as that for the reaction over the Zn-deposited Cu surface, the catalyst was exposed to a N_2O/He (2.5%) gas stream without exposure to air. From the amount of N_2 formed by the reaction of N_2O with metallic Cu, the amount of metallic Cu during methanol synthesis (Cu_{react}) could be estimated, which was then compared to the amount of metallic Cu after rereducing the postreaction catalyst with H_2 at 523 K and 18 atm (Cu_{total}). Based on the measurements of Cu_{react} and Cu_{total}, oxygen coverage on the Cu surface for the postreaction catalysts was calculated. The TOF of CO_2 hydrogenation for the powder catalysts was obtained by carrying out the reaction with small *W/F* values varying from 3×10^{-5} to 2×10^{-4} g cat min/cc to obtain the reaction rates at low conversions, where *W* and *F* stand for the catalyst weight (g) and the flow rate (cc/min), respectively.

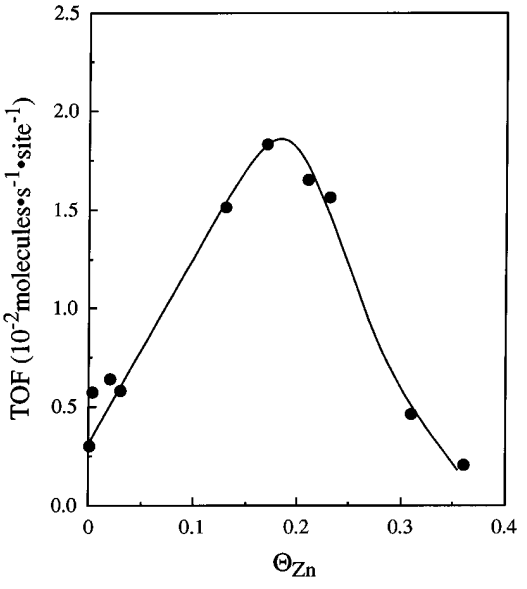

FIG. 2. TOF for methanol formation on the Zn-deposited Cu surface as a function of Zn coverage. The hydrogenation of CO_2 was carried out at 523 K and 18 atm. The Zn coverage was measured after the reaction using XPS.

III. RESULTS

III.1. Methanol Synthesis over ZnO_x/Cu Model Catalysts vs Cu Powder Catalysts

The hydrogenation of CO_2 over the Zn-deposited Cu surface was carried out at 523 K and 18 atm with variation of the Zn coverage estimated using XPS after the reaction. The reaction reached a steady state within 30 min, and no deactivation of the catalyst was observed for 3 h after the steady state. Figure 2 shows the TOFs for methanol formation at 523 K as a function of the Zn coverage. It is shown that the TOF increased with Zn coverage below $\Theta_{Zn} = 0.17$ and that the TOF decreased above $\Theta_{Zn} = 0.17$. This indicates the formation of active sites. At the optimum coverage, the Zn-deposited Cu surface was six times more active for methanol formation than the Zn-free polycrystalline Cu surface. These results clearly indicated that the adsorbed ZnO_x species formed on the Cu surface during the reaction directly promotes methanol synthesis. The decrease in the activity above $\Theta_{Zn} = 0.2$ is discussed later based on the results of the postreaction surface analysis (Sections III.2.3 and IV.1). The yield of methanol is on the order of 3×10^{-4}% at a TOF of 1.8×10^{-2} molecules $site^{-1}$ s^{-1}, which is much less than the equilibrium conversion of 6.2%, implying that the reaction is far from the equilibrium. The data were quite reproducible regardless of the sample history if the Zn coverage was the same.

The results shown in Fig. 2 are very similar to the mountain-shaped relation between methanol synthesis activity and oxygen coverage previously obtained for the Cu-based catalysts (15). On the Zn-deposited Cu surface, oxygen was detected by postreaction surface analysis (see Section III.2.1.), which is due to the reaction mixture. Thus, the relationship with oxygen coverage was examined for the ZnO_x/Cu model catalyst in comparison with the results of the Cu-based powder catalysts, Cu/ZnO, Cu/SiO_2, and Cu/Ga_2O_3. Figure 3 shows the TOF as a function of oxygen coverage for the Zn-deposited Cu surface and Cu-based powder catalysts. The very similar mountain-shaped curve for the Zn-deposited model catalyst was obtained as previously observed for the powder catalysts, where the maximum activity appeared at an oxygen coverage of ~0.17. Furthermore, the value of the TOF for the Zn-deposited Cu surface is in agreement with that for the powder Cu catalysts. Thus, it is concluded that both systems have essentially the same catalytic nature and that the Zn-deposited Cu model catalyst reveals the real features of the industrial Cu catalyst. Further, the relationship can be applied to any Cu catalysts containing different metal oxides as reported previously, so that the present model Cu catalyst can serve as a study of the support effect.

Figure 4 shows Arrhenius plots for methanol formation over the Zn-deposited Cu model catalyst and the Cu/ZnO (50/50) catalysts. The oxygen coverage for the Zn-deposited Cu catalyst was $\Theta_O = 0.17$, the optimum coverage, while the oxygen coverage for the Cu/ZnO catalyst was $\Theta_O = 0.23$ at which the activity is slightly less than the maximum (by ~30%). From the slopes of the lines shown in Fig. 4, the apparent activation energies for methanol formation over the Zn-deposited Cu model catalyst and the

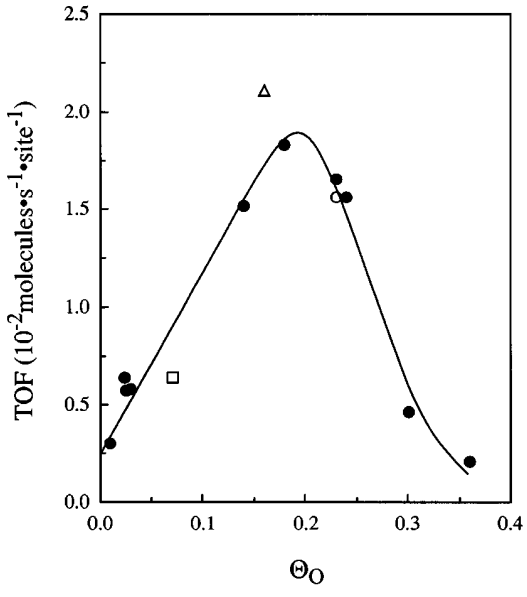

FIG. 3. TOF for methanol formation as a function of oxygen coverage for the Zn-deposited Cu surface (●), Cu/ZnO (○), Cu/SiO_2 (□), and Cu/Ga_2O_3 (△). The hydrogenation of CO_2 was carried out at 523 K and 18 atm. The Zn coverage was measured after the reaction using XPS.

Cu/ZnO (50/50) catalyst are 76.3 ± 4.0 and 69.3 ± 3.6 kJ/mol, respectively. Considering the difference in oxygen coverage, the agreement of the TOF between the model catalyst and the Cu powder catalysts is fairly good. This also supports the applicability of the model catalyst.

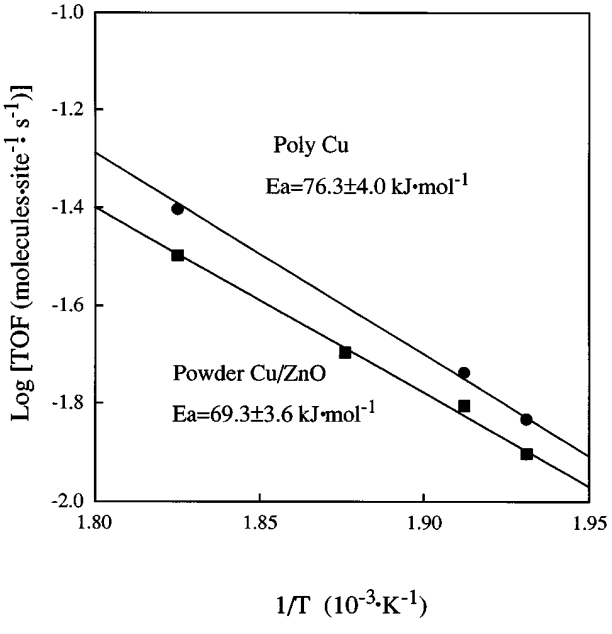

FIG. 4. Arrhenius plot for methanol formation over the Zn-deposited Cu model catalyst and the Cu/ZnO (50/50) catalyst. The oxygen coverage for the Zn-deposited Cu catalyst and the Cu/ZnO catalyst were 0.17 and 0.23, respectively.

The reverse water–gas shift (RWGS) reaction, $CO_2 + H_2 \rightarrow CO + H_2O$, also occurred on the Zn-deposited and Zn-free Cu polycrystalline surfaces, as proved by the formation of CO. Although the exact conversion was not obtained because of the contribution of the wall irregularly catalyzing the RWGS reaction, no promotional effect of ZnO deposited on the Cu surface was observed, indicating that the ZnO_x species is not an essential species for the RWGS reaction.

III.2. Postreaction Surface Analysis

III.2.1. Zn 2p, O 1s. The surface analysis by XPS was carried out after deposition of Zn and the hydrogenation of CO_2 at room temperature. For the postreaction analysis, the reactant gas was evacuated in the preparation chamber while the sample was maintained at ~523 K (heating current off), and then the XPS measurements were made in the UHV analysis chamber. Thus, surface species adsorbed stably at ~523 K can be detected, or the species formed by the decomposition may be detected in the postreaction surface analysis.

Figures 5 and 6 show the Zn $2p_{3/2}$ and O 1s spectra, respectively, of the surface before and after the reaction for the Zn-deposited Cu surface with a Zn coverage of $\Theta_{Zn} = 0.17$. It was found that the Zn $2p_{3/2}$ peak at 1021.7 eV for the postreaction surface is higher in binding energy than that for the initially deposited Zn atoms on the clean Cu surface by ~0.6 eV. The binding energy of the Zn $2p_{3/2}$ peak observed before reaction was always 1021.1–1021.2 eV regardless of the Zn coverage. Because oxygen was nearly absent on the clean Cu surface before the reaction (see Fig. 6), the Zn $2p_{3/2}$ peak at 1021.1 eV was attributed to Zn metal atoms, which value was slightly less than the literature value (1021.4 V) (19). On the other hand, the Zn $2p_{3/2}$ peak at 1021.7 eV was assigned to Zn ions combined with oxygen seen in the O 1s spectra after the reaction (Fig. 6), where the binding energy was very close to that for bulk ZnO (1021.6–1021.7 eV) (20, 21). Further, the binding energy of the O 1s peak at 530.7 eV for the postreaction surface was close to that for the oxygen in a ZnO crystal (530.5–530.6 eV) (20, 22). It is known that the binding energy of O 1s for the oxygen on the Cu surface is 529.4–530.0 eV (20, 23–25). The binding energy of O 1s for the oxygen adsorbed on the poly-Cu clean surface was determined to be 530.0 eV in this study. Thus, it was considered that the oxygen formed on the Zn-deposited surface was preferentially bound to the Zn ions on the Cu surface. The peak widths for Zn $2p_{3/2}$ was 2.18 eV for $\Theta_{Zn} = 0.17$ and 2.29 eV for $\Theta_{Zn} = 0.23$, which are significantly larger than that for initially-deposited metallic Zn (1.86 eV). This suggests that the ZnO_x species is a mixture of ZnO and metallic Zn.

The shoulder O 1s peak at 533 eV (~6% of the main peak) was assigned to formate species based on the BE and the thermal stability as discussed in Section III.2.3.

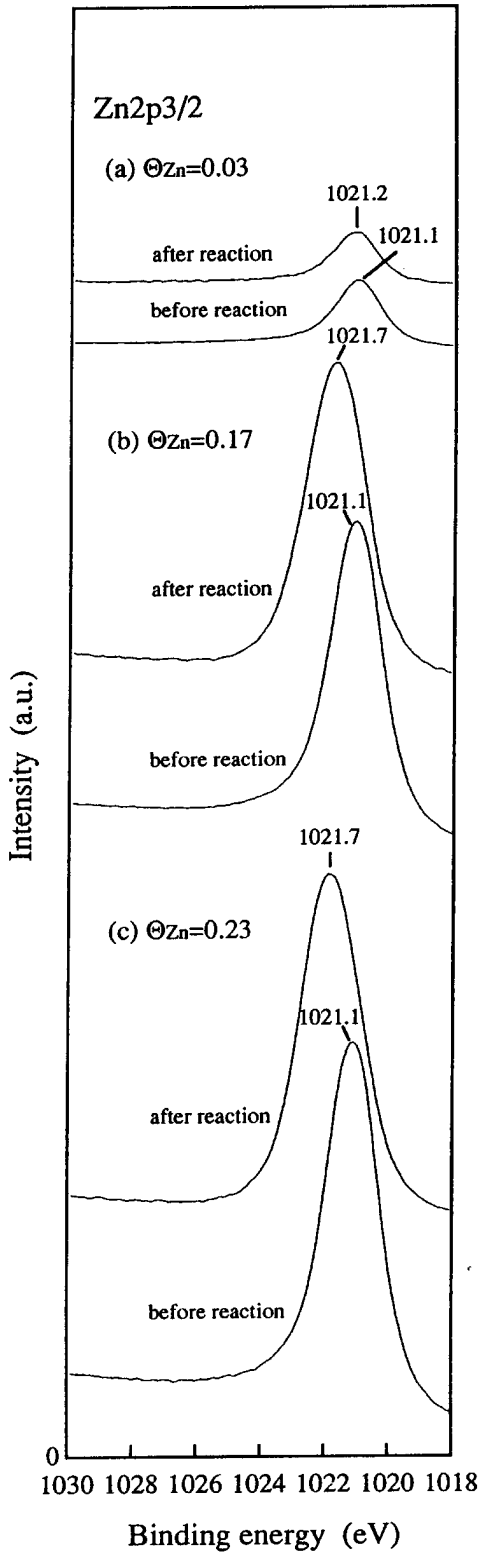

FIG. 5. XPS spectra of Zn $2p_{3/2}$ for the Zn-deposited Cu surface with various Zn coverage, taken before and after reaction.

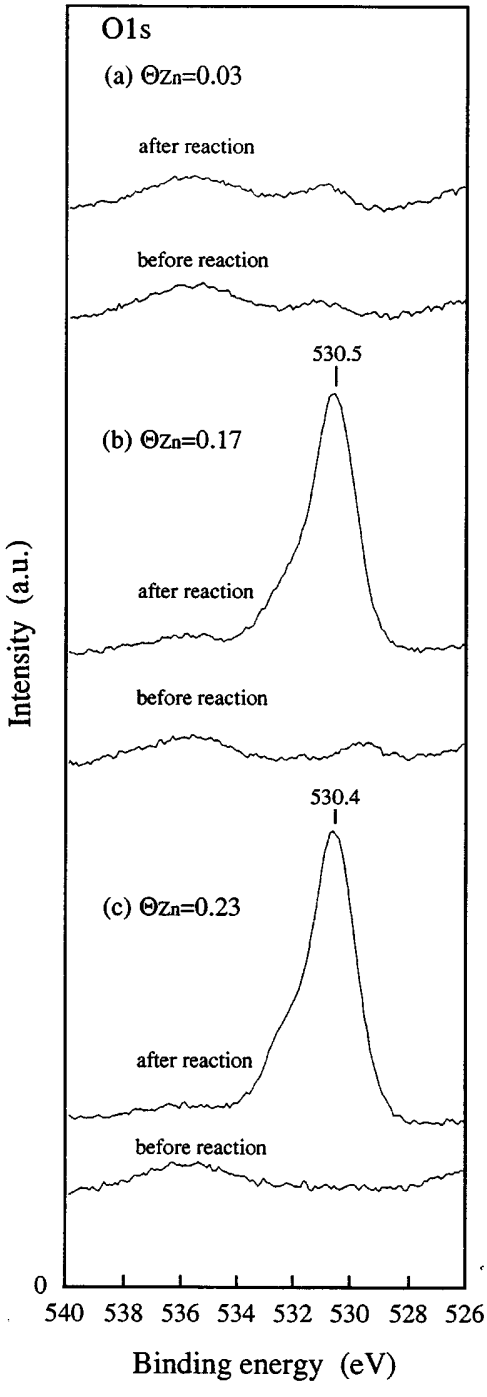

FIG. 6. XPS spectra of O 1s for the Zn-deposited Cu surface with various Zn coverage, taken before and after reaction.

Figure 7 shows the coverages of oxygen and Zn estimated using sensitivity factors as described in the experimental section. The oxygen coverage was found to be equal to the Zn coverage in the range between $\Theta_{Zn} = 0$ and $\Theta_{Zn} = 0.4$, indicating the formation of ZnO independent of the coverage. However, it is possible that the oxygen is formed by decomposition of intermediates upon evacuation at 523 K.

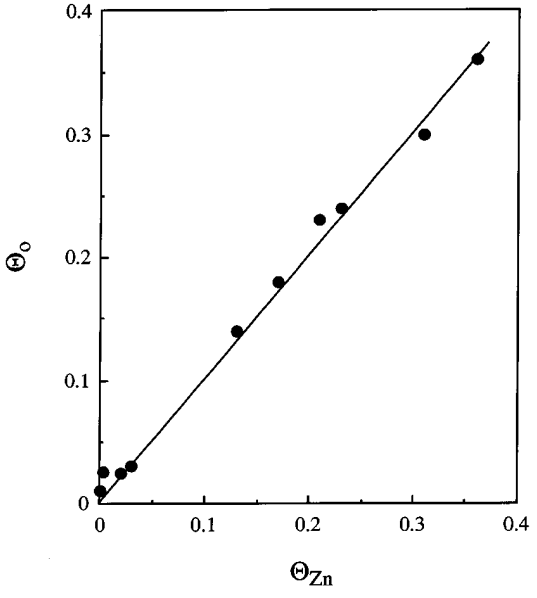

FIG. 7. Oxygen coverage versus Zn coverage for the postreaction Zn-deposited Cu surfaces.

No oxygen adsorbed on the Zn-free Cu surface was observed, indicating that the steady-state coverage of the oxygen formed on the metallic Cu surface is very small. This is because the oxygen on Cu is readily reduced by H_2. The results shown in Figs. 5–7 thus suggest that the oxygen is bound to Zn atoms more strongly than to Cu atoms.

III.2.2. Cu 2p. Figure 8 shows Cu $2p_{3/2}$ spectra for the clean and the Zn-deposited Cu surfaces ($\Theta_{Zn} = 0, 0.17, 0.23$) taken before and after the reaction. It was found that the Cu $2p_{3/2}$ peak for the postreaction Cu surface slightly shifted to lower energies by ~0.2 eV, compared to that of the clean Cu surface (932.4 eV). The shift was more prominent with increasing Θ_{Zn}. It is known that the Cu $2p_{3/2}$ peak for Cu_2O has a slightly lower binding energy than that for Cu, while the Cu $2p_{3/2}$ peak for CuO has a higher binding energy than that for Cu (19, 26). Jernigan and Somorjai (26) have reported that the Cu $2p_{3/2}$ peak for Cu_2O is lower than that for Cu by 0.2 eV, although their absolute binding energies (Cu $2p_{3/2}$ for metallic Cu; 932.8 eV) seem to be higher than normal values by ~0.4 eV. Thus, the slight shift to low binding energies in Fig. 8 is probably due to formation of Cu^+ species similar to Cu_2O. No satellite peak around the Cu $2p_{3/2}$ peak, characteristic of CuO, was observed for the postreaction surface. Taking into consideration that the oxygen observed on the postreaction Cu surface is stabilized by Zn as described above, the Cu^+ species is probably formed in the vicinity of the ZnO species.

III.2.3. C 1s. Figure 9 shows C 1s spectra for the Zn-deposited Cu surface ($\Theta_{Zn} = 0.17$), taken before and after the reaction. Two peaks were seen at 284.8 and 289.2 eV in the spectrum after the reaction. The former was attributed to graphitic carbon deposited during or after the reaction based on the BE, which is probably due to the small amount of hydrocarbon formed by the hydrogenation of CO catalyzed by the reactor wall described in the experimental section. The coverage of surface graphitic car-

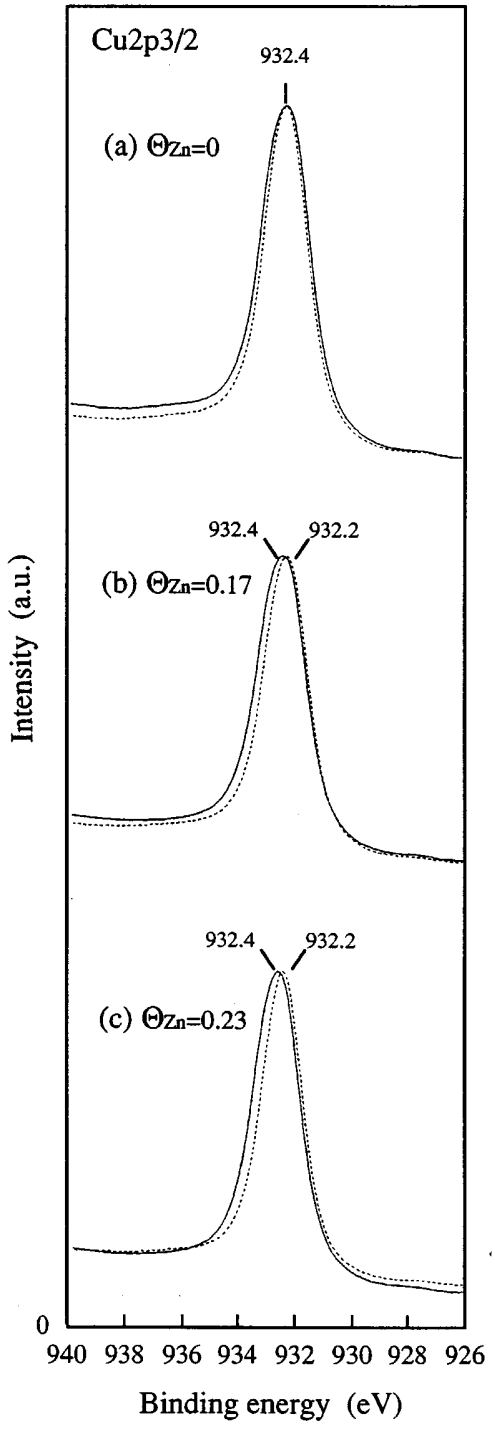

FIG. 8. XPS spectra of Cu $2p_{3/2}$ for the Zn-deposited Cu surface with various Zn coverage, taken before (solid line) and after (broken line) reaction.

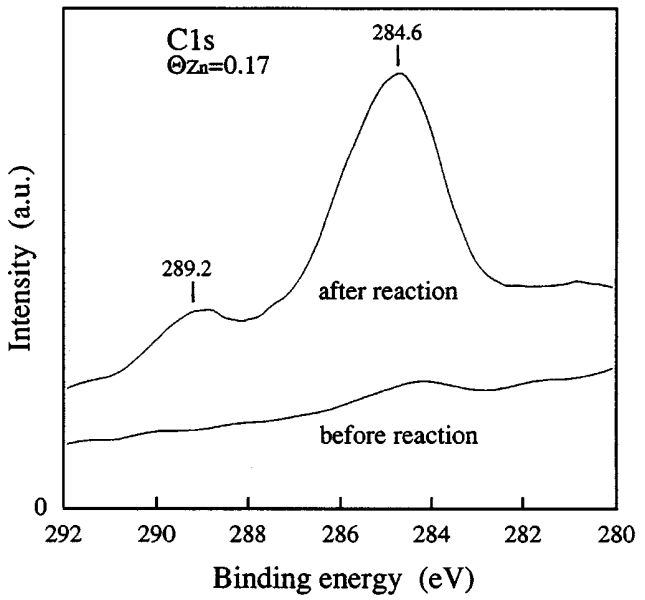

FIG. 9. XPS spectra of C 1s for the Zn-deposited Cu surface ($\Theta_{Zn} = 0.17$), taken before and after reaction.

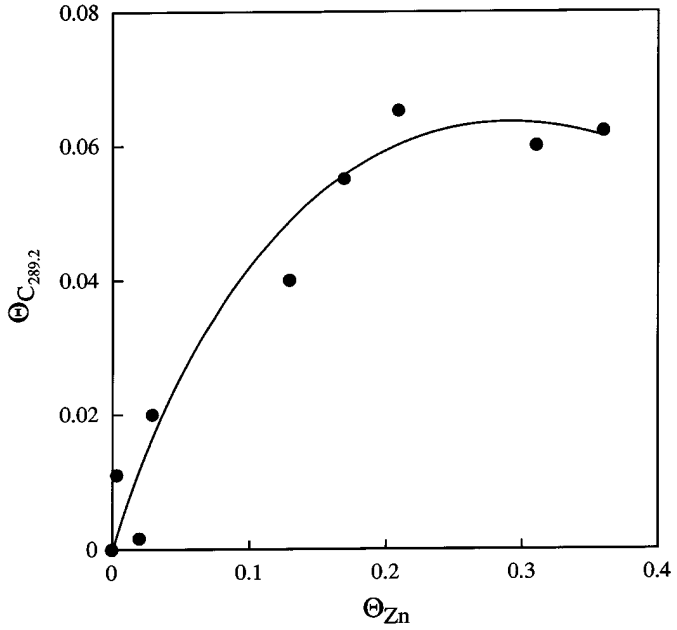

FIG. 10. Formate coverage versus Zn coverage for the postreaction Zn-deposited Cu surfaces.

bon was estimated to be $\Theta_C = 0.1$–0.2, regardless of the Zn coverage. The catalytic activity decreased from 0.46 to 0.42 in TOF when the carbon coverage increased from $\Theta_C = 0.12$ to $\Theta_C = 0.18$. Thus, TOF shown in Figs. 2 and 3 should be less than for a carbon-free Cu by 10–20 %. The carbon deposition tended to be more significant at higher reaction temperatures.

On the other hand, the C 1s peak at 289.2 eV in Fig. 9 was attributed to carbon-containing intermediates of methanol synthesis. It has been reported that formate and methoxy species adsorbed on Cu catalysts are observed by *in situ* FT-IR during methanol synthesis reaction by CO_2 hydrogenation. Based on the binding energy, the thermal stability, and the formation conditions (temperature or pressure), the peak at 289.2 eV was assigned to the formate species (see Section IV.3.).

Figure 10 shows the coverage of the formate species estimated from the area of the peak at 289.2 eV as a function of Zn coverage on the Cu surface. It is clear that the formate coverage increases with the Zn coverage between $\Theta_{Zn} = 0$ and 0.4, indicating that the formate species is stabilized by the ZnO_x species on the Cu surface. This suggests that the role of the active sites for methanol synthesis should be to stabilize the formate intermediates, which clearly explains that the rate determining step of methanol synthesis, in the hydrogenation of CO_2 over a Cu/ZnO catalyst, is the hydrogenation of the formate to the methoxy species (27). The feature in the relation between Θ_C and Θ_{Zn} is, however, different from that between TOF and Θ_{Zn}, i.e., the mountain-shaped relationship shown in Fig. 2; thus, the activity cannot be explained only by the amount of the formate intermediates. That is, metallic Cu is also necessary in methanol synthesis for elemental steps such as dissociative adsorption of H_2, as suggested by the results for methanol synthesis over the Cu-based powder catalysts (15–17).

The decomposition of the carbonaceous species formed on the postreaction surface was examined, where XPS spectra were taken while the sample was heated in UHV. It took ~30 min for each XPS measurement and heating at a certain temperature. As shown in Fig. 11, the formate species with the C 1s BE of 289.2 eV decomposed at ~573 K, which is higher than the decomposition temperature of the formate on metallic Cu by ~100 K even at a much smaller heating rate. Again, it is suggested that the formate species is bound to the ZnO_x species on the Cu surface.

IV. DISCUSSION

IV.1. Creation of the New Active Sites

It this study, it was clearly shown that the ZnO_x species on the Cu surface directly promoted the methanol formation activity. The optimum TOF of the Zn-deposited Cu was very close to that for the Cu/ZnO powder catalyst, which was higher than the TOF for the clean Cu surface by a factor of 6 (Fig. 2). Although some researchers have reported that the activity of Cu catalysts is determined only by the surface area of the metallic Cu (6–9), the present study definitely showed the creation of new active sites, except for Cu^0, as seen in the increase in activity upon covering the ZnO_x on Cu in spite of the resulting decrease in the surface area of the metallic Cu.

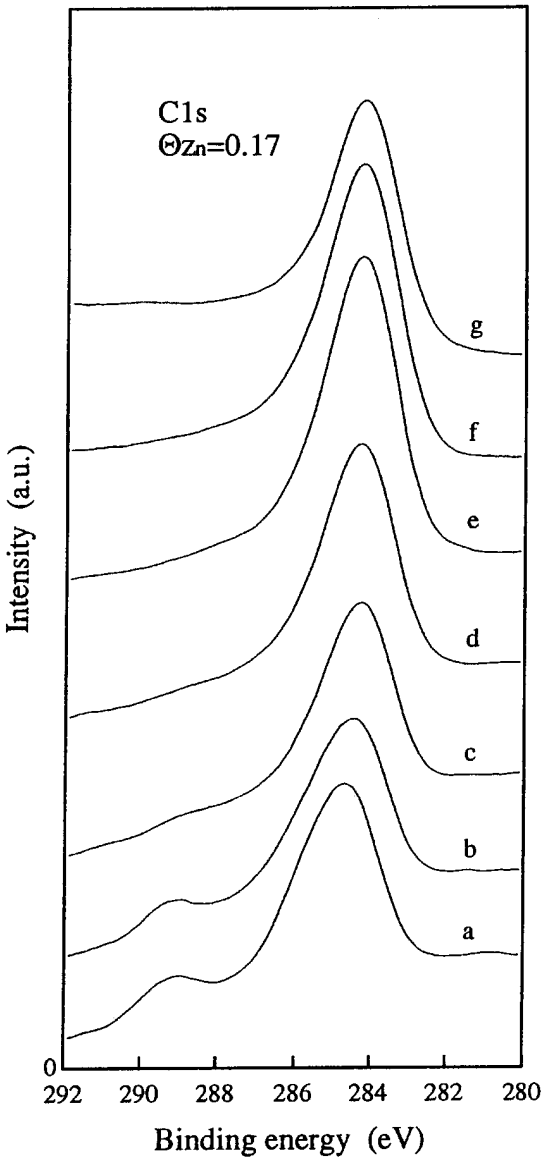

FIG. 11. Change in C 1s spectra upon heating the postreaction Zn-deposited Cu surface ($\Theta_{Zn} = 0.17$) in UHV: (a) 523 K, (b) 573 K, (c) 623 K, (d) 673 K, (e) 723 K, (f) 773 K, (g) 823 K.

The active sites may be attributed to Cu^+ in the vicinity of the ZnO_x species, which has been previously suggested in our studies of the Cu-based powder catalysts (15–17). That is, high-temperature reduction of a physical mixture of ZnO/SiO_2 and Cu/SiO_2 with H_2 resulted in an increase in specific activity for methanol formation accompanying an increase in the oxygen coverage on the Cu surface of the postreaction catalyst (17). These facts were found to be due to the migration of ZnO_x species from ZnO particles onto Cu particles upon hydrogen reduction by EDX–TEM measurements. Thus, the Cu^+-O-Zn species has been proposed to be the active species, created in the vicinity of the ZnO_x species on the Cu surface. The promotional model of the ZnO_x species on Cu was directly confirmed in this study. Further, the existence of the Cu^+ species was shown in the measurements of Cu $2p_{3/2}$ spectra after reaction. Thus, we considered that the role of the ZnO_x species is to create an active species such as Cu^+-O-Zn in the vicinity of ZnO_x species.

Existence of special sites in Cu-based methanol synthesis catalysts has been reported in many literature sources since Klier and co-workers (3) proposed that isolated Cu^+ ions on the surface of ZnO are the active site for the methanol synthesis based on the results of UV measurements. Later, Parris and Klier (28) reported that irreversible adsorption of CO at 293 K occurs on the isolated Cu^+, where they showed correlation between the methanol synthesis activity and the amount of the irreversible adsorbed CO. Furthermore, there has been some spectroscopic evidence for the presence of Cu^+ species. Okamoto *et al.* (29) have used X-ray induced auger electron spectroscopy to identify Cu^+ separately from Cu^0 for reduced CuO–ZnO catalysts, where $Cu(L_3M_{4,5}M_{4,5})$ peaks for Cu^0 and Cu^+ appeared at 918.4 and 916.7 eV, respectively. King and co-workers have characterized unsupported alkali-promoted copper catalysts ($CuLi_{0.5}$, $CuNa_{0.5}$, $CuK_{0.5}$, $CuRb_{0.5}$, and $CuCs_{0.5}$) using NMR (5) and XPS (30). The NMR spectra of ^{65}Cu showed the presence of "Cu^+-like species" whose amount correlated with the catalytic activity for the methanol synthesis by the hydrogenation of CO. ^{133}Cs NMR spectra further indicated the formation of cesium carbonate. They concluded that the promotional effect of alkali addition was due to the stabilization of the Cu^+ species present in the alkali carbonate framework. As for the surface science approach using a clean Cu surface, Szanyi and Goodman (4) have reported that the very low concentration of ionic copper species on the Cu(100) clean surface is responsible for the low activity of the Cu(100) catalyst. They have also pointed out that the impurities present on the Cu surface serve as promoters to enhance the concentration of ionic copper. Chan and Griffin (31) have reported the presence of Cu cation sites in a model catalyst where Cu is evaporated on RF plasma-grown ZnO thin films and shown that $HCOO_a$ species adsorbed on the Cu cations is more stable than on metallic Cu clusters. These Cu active ion species reported in the above literature sources are considered to be identical with the species observed in this study.

The importance of the results in Fig. 3 also lies in the point that metallic copper atoms are also necessary for catalyzing methanol synthesis, as shown by the mountain-shaped relation between TOF and oxygen coverage. That is, the TOF was found to be decreased with the coverage of the ZnO_x above $\Theta_{Zn} = 0.19$, which is due to a decrease in the surface area of metallic Cu. The role of Cu^0 is probably to dissociate H_2 for hydrogenation steps. On the other hand, Cu^+ species may stabilize the intermediates such as formate or

methoxy species. Thus, the Zn-deposited active Cu surface may possess a bifunctional catalytic property.

We consider that Cu^0 itself is less active than the ZnO_x promoted Cu surfaces or the catalytic component in Cu/ZnO catalysts for methanol synthesis based on the literature results and our powder Cu/SiO_2 data. Namely, no activity of impurity-free Cu/SiO_2 (30, 32) has been reported in the hydrogenation of CO or CO/CO_2 or CO_2. Further, the low activity of Cu^0 may be attributed to the small amount of defects, which creates stable adsorbed oxygen atoms as well as Cu^+ species.

IV.2. Reaction Intermediates

The carbon-containing species with the C 1s BE of 289.2 eV detected on the postreaction surface may be related to the reaction intermediates for methanol formation because the coverage of the carbon-containing species increases with Zn coverage as well as TOF as seen in Figs. 2 and 10. The assignments of the C 1s and O 1s (~533 eV) peaks were made based on the literature data of XPS, FT-IR, and TPD studies concerning methoxy, formate, and carbonate species, which have been regarded as possible intermediates for the methanol synthesis. It is known that the C 1s BE in the range of 287.7–289.5 eV can assigned to carbonate or formate adspecies (33), while the methoxy species has a BE of 286.2–287.2 eV on ZnO(34), O/Cu(111), Fe, Pd, and MgO (33). As for *in situ* FT-IR studies, formate and methoxy species have been observed on Cu/ZnO catalysts during the methanol synthesis by the hydrogenation of CO_2 (+CO). Thus, we assigned the C 1s peak at 289.2 eV to the formate species.

It was shown that the formate species decomposed at ~500 K when heated in UHV (Fig. 11), which was higher than the decomposition temperature of the formate on metallic Cu surfaces. In TPD experiments with the formate species on Cu(110) and Cu(111), CO_2 and H_2 desorb with peak at ~480 K at a heating rate of 2–5 K/s (18, 35–37). On ZnO surfaces, the formate species will decompose at higher temperatures of 570–580 K at a heating rate of 0.7 K/s (38, 39). Although the decomposition temperature of the formate in this study (~573 K) is close to that of the formate on ZnO, we speculate that the formate species forms on the active sites created in the vicinity of the ZnO_x species, because the coverage of the formate increased with Zn coverage as well as TOF for the methanol synthesis. Because the rate determining step for methanol synthesis has been considered to be the hydrogenation of formate to methoxy species, the amount of stable formate should determine the net reaction rate. This has also been discussed in the studies of the physical mixture of Cu/SiO_2 and ZnO/SiO_2, and the results are consistent with the present results.

It should be noted that the intermediates species, which were not detected in this study because of the decomposition upon evacuation of the reaction mixture at 523 K, will exist during the hydrogenation of CO_2 on the Zn-deposited Cu surface. The formate species on metallic Cu has been observed under the reaction condition by *in situ* FT-IR (27, 40, 41). In this study, the formate on Cu^0 was considered to be completely decomposed to CO_2 and H_2 without leaving any species on the surface. There is a possibility that the formate species detected on the postreaction surface is formed upon evacuation by the decomposition of methoxy intermediates. Currently, it is not clear whether the formate is formed during reaction or during evacuation. Whichever the case is, the intermediate anions ($HCOO^-$ or CH_3O^-) are considered to be stabilized by the ZnO_x species, leading to the promotional effect on methanol synthesis.

IV.3. Kinetics

Kinetic measurements of the methanol synthesis on the surface of a Cu single crystal have been attempted in the hydrogenation of CO ($+CO_2$) (4) and the hydrogenation of CO_2 (9, 42). Chorkendorff and co-workers (9) have reported that the turnover frequency for methanol formation on a clean Cu(100) surface is 2.7×10^{-4} (site s)$^{-1}$ at a total pressure of 2 atm ($CO_2:H_2$, 1:1) and 543 K, and the apparent activation energy is 69 kJ/mol. They considered that the metallic Cu is the active catalyst and the role of ZnO is then one of determining the degree of Cu dispersion, which strikingly contrasts with our conclusions. However, the activation energy is similar to the activation energy for the Zn coverage of 0.17 (76 kJ/mol) in this study. Further, the turnover frequency is comparable to that for the *Zn-free* Cu polycrystalline surface obtained in this study, i.e, 3×10^{-3} molecules site^{-1} s^{-1} at 523 K and 18 atm, assuming a first-order dependence of the turnover frequency on the total pressure.

On the other hand, the turnover frequency of methanol formation by the hydrogenation of CO is considerably low compared to that for the hydrogenation of CO_2. Szanyi and Goodman (4) have reported a turnover frequency of 1.3×10^{-7} molecules site^{-1} s^{-1} for methanol formation on a clean Cu(100) surface at 525 K and 750 Torr using a gas mixture of $CO_2/CO/H_2 = 1/2/12$, which is three orders of magnitude lower than that for CO_2 hydrogenation obtained by Chorkendorff and co-workers (9). The difference in TOF is probably due to a redox condition where CO and H_2 are reductants removing surface oxygen while CO_2 is an oxidant supplying surface oxygen.

V. CONCLUSIONS

(1) The hydrogenation of CO_2 over a Zn-deposited polycrystalline surface was carried out at 523 K and 18 atm in a high pressure reactor connected to an XPS–AES apparatus. At optimum Zn coverage ($\Theta_{Zn} = 0.17$) the Zn-deposited Cu surface was six times more active than the Zn-free Cu surface for methanol formation, indicating the formation of

active sites except for Cu^0. The TOF increased with Zn coverage below $\Theta_{Zn} = 0.17$ and decreased above $\Theta_{Zn} = 0.17$.

(2) The TOF and the activation energy for methanol formation over the Zn-deposited Cu were in fairly good agreement with those for the Cu/ZnO powder catalysts; thus, it is reasonable to regard the Zn-deposited Cu as a model of Cu/ZnO catalysts. Also, we observed a mountain-shaped relationship between oxygen coverage on the postreaction Cu surface and TOF for methanol formation very similar to that for supported Cu catalysts.

(3) The postreaction surface analysis by XPS clearly showed the formation of ZnO species with a Zn/O ratio of unity at any Zn coverage. The Zn $2p_{3/2}$ peak appeared at 1021.7, which is equal to that for bulk ZnO. Also Cu^+ species was observed on the postreaction Cu surface in the presence of ZnO_x species.

(4) The formate species was observed on the postreaction Zn-deposited Cu surface, which increased with Θ_{Zn} below $\Theta_{Zn} = 0.2$ and then slightly decreased at $\Theta_{Zn} > 0.2$. It is suggested that the role of the active ZnO_x species is due to the stabilization of the intermediates such as formate or methoxy species.

ACKNOWLEDGMENT

This work was partly supported by New Energy and Industrial Technology Development Organization.

REFERENCES

1. Bart, J. C. J., and Sneeden, R. P. A., *Catal. Today* **2**, 1 (1987).
2. Chinchen, G. C., Denny, P. J., Jennings, J. R., Spencer, M. S., and Waugh, K. C., *Appl. Catal.* **36**, 1 (1988).
3. Klier, K., *Adv. Catal.* **31**, 243 (1982).
4. Szanyi, J., and Goodman, D. W., *Catal. Lett.* **10**, 383 (1991).
5. Chu, P., Gerstein, B. C., Sheffer, G. R., and King, T. S., *J. Catal.* **115**, 194 (1989).
6. Chinchen, G. C., Spencer, M. S., Waugh, K. C., and Whan, D. A., *J. Chem. Soc. Faraday Trans.* **83**, 2193 (1987).
7. Chinchen, G. C., Waugh, K. C., and Whan, D. A., *Appl. Catal.* **25**, 101 (1986).
8. Pan, W. X., Cao, R., Roberts, D. L., and Griffin, G. L., *J. Catal.* **114**, 440 (1988).
9. Rasmussen, P. B., Holmblad, P. M., Askgaard, C. V., Ovesen, C. V., Stoltze, P., Norskov, J. K., and Chorkendorff, I., *Catal. Lett.* **26**, 373 (1994).
10. Didziulis, S. V., Butcher, K. D., Cohen, S. L., and Solomon, E. I., *J. Am. Chem. Soc.* **111**, 7110 (1989).
11. Ludviksson, A., Ernst, K. H., Zhang, R., and Campbell, C. T., *J. Catal.* **141**, 380 (1993).
12. Burch, R., Chappel, R. J., and Golunski, S. E., *J. Chem. Soc. Faraday Trans. 1* **85**, 3569 (1989).
13. Burch, R., Golunski, S. E., and Spencer, M. S., *J. Chem. Soc. Faraday Trans.* **86**, 2683 (1990).
14. Frost, J. C., *Nature* **334**, 577 (1988).
15. Fujitani, T., Saito, M., Kanai, Y., Kakumoto, T., Watanabe, T., Nakamura, J., and Uchijima, T., *Catal. Lett.* **25**, 271 (1994).
16. Kanai, Y., Watanabe, T., Fujitani, T., Saito, M., Nakamura, J., and Uchijima, T., *Catal. Lett.* **27**, 67 (1994).
17. Kanai, Y., Watanabe, T., Fujitani, M., Nakamura, J., and Uchijima, T., *Catal. Lett.,* in press.
18. Russell, J. N., Jr., Gates, S. M., and Yates, J. T., Jr., *Surf. Sci.* **163**, 516 (1985).
19. Muilenberg, G. E. (Ed.), "Handbook of X-Ray Photoelectron Spectroscopy." Perkin-Elmer, Eden Prairie, MN, 1979.
20. Campbell, C. T., Daube, K. A., and White, J. M., *Surf. Sci.* **182**, 458 (1987).
21. Vohs, J. M., and Barteau, M. A., *Surf. Sci.* **176**, 91 (1986).
22. Au, C. T., Hirsch, W., and Hirschwald, W., *Surf. Sci.* **197**, 391 (1988).
23. Gruzalski, G. R., Zehner, D. M., and Wendelken, J. F., *Surf. Sci.* **159**, 353 (1985).
24. Clendening, W. D., Rodriguez, J. A., Campbell, J. M., and Campbell, C. T., *Surf. Sci.* **216**, 429 (1989).
25. Brundle, C. R., *Faraday Discuss. Chem. Soc.* **60**, 159 (1975).
26. Jernigan, G. G., and Somorjai, G. A., *J. Catal.* **147**, 567 (1994).
27. Fujita, S., Usui, M., Ohara, E., and Takezawa, N., *Catal. Lett.* **13**, 349 (1992).
28. Parris, G. E., and Klier, K., *J. Catal.* **97**, 374 (1986).
29. Okamoto, Y., Fukino, K., Imanaka, T., and Teranishi, S., *J. Phys. Chem.* **87**, 3747 (1983).
30. Sheffer, G. R., and King, T. S., *J. Catal.* **116**, 488 (1989).
31. Chan, L., and Griffin, G. L., *Surf. Sci.* **173**, 160 (1986).
32. Nonneman, L. E. Y., and Ponec, V., *Catal. Lett.* **7**, 213 (1990).
33. Peng, X. D., and Barteau, M. A., *Surf. Sci.* **224**, 327 (1989).
34. Au, C. T., Hirsch, W., and Hirschwald, W., *Surf. Sci.* **221**, 113 (1989).
35. Bowker, M., and Madix, R. J., *Surf. Sci.* **102**, 542 (1981).
36. Sexton, B. A., Hughes, A. E., and Avery, N. R., *Surf. Sci.* **155**, 366 (1985).
37. Wachs, I., and Madix, R. J., *J. Catal.* **53**, 208 (1978).
38. Vohs, J. M., and Barteau, M. A., *Surf. Sci.* **197**, 109 (1988).
39. Bowker, M., Houghton, H., and Waugh, K. C., *J. Chem. Soc. Faraday Trans. 1* **77**, 3023 (1981).
40. Neophytides, S. G., Marchi, A. J., and Froment, G. F., *Appl. Catal.* **A 86**, 45 (1992).
41. Saussey, J., and Lavalley, J. C., *J. Mol. Catal.* **50**, 343 (1989).
42. Rasmussen, P. B., Kazuta, M., and Chorkendorff, I., *Surf. Sci.* **318**, 267 (1994).